

## Light scattering by injection molded particle filled polymers

Eugenio R. Méndez<sup>a</sup>, Rubén G. Barrera<sup>b</sup>, Roberto Alexander-Katz<sup>c</sup>

<sup>a</sup>*División de Física Aplicada/CICESE, Apartado Postal 2732, 22800 Ensenada B.C., Mexico*

<sup>b</sup>*Instituto de Física/UNAM, Apdo. Postal 20-364, 01000 México D.F., Mexico*

<sup>c</sup>*Area de Polímeros, Depto. de Física, UAM-I, Apdo. Postal 55-534, 09340 México D.F., Mexico*

---

### Abstract

A study of light scattering by surfaces of injection molded particle filled polymers is presented. In particular the effect that molding conditions have on surface roughness is studied by mechanical and optical profilometry as well as by light scattering. It is shown that Kirchhoff scalar theory with a Gaussian probability density of heights and a negative exponential correlation function between heights predicts reasonably well the surface scattering properties in an angular interval around the specular angle for all the molding conditions studied. This leads to a simple analytical model for gloss with only two parameters.

---

### 1. Introduction

Engineering plastics are used in many products ranging from electrodomestic household goods to applications in car and computer industries. In many cases, surface related optical properties such as gloss have to be controlled to fulfill functional or appearance specifications. Many of these materials are particle filled, and the gloss of the objects made out of them is strongly influenced by the migration of particles to the surface and the smoothing at the mold wall [1–5]. The kinetics of such mechanisms is governed by molding conditions as well as material properties such as particle size distribution, matrix viscosity, and surface tension [2,3,5]. Therefore, surface roughness of a final product is not only dependent on material properties but will be highly sensitive to process variables. The purpose of the present study is to determine if there is an optical model for particle filled plastics that is able to describe the scattering properties around the specular angle for all molding conditions. With that object in mind, we performed a detailed surface characterization by mechanical and optical profilometry and

compared the theoretically generated scattering patterns with actual light scattering data.

## 2. Experimental procedures

### 2.1. Materials

For this study we have chosen a typical formulation of an ABS resin (acrylonitrile-butadiene-styrene polymer) and a model system consisting of a matrix of poly(styrene-co-acrylonitrile) and 4% by volume of rubber particles of poly(butadiene-styrene-acrylonitrile) with a weight-average diameter of  $\bar{D}_w = 0.851 \mu\text{m}$  and a number-average diameter  $\bar{D}_n = 0.59 \mu\text{m}$ . The mixing was done by means of a Banbury machine and afterwards injection molded with an Engel molding machine model ES-330/85. Mold temperature was set at  $40^\circ\text{C}$  while the stock temperatures (temperature of the polymer melt) measured at the nozzle were  $207 \pm 2.08^\circ\text{C}$  (low),  $235 \pm 1^\circ\text{C}$  (medium) and  $247 \pm 1.5^\circ\text{C}$  (high). The injection rates used were 0.76 (low), 1.5 (medium) and 3 cm/s (high). From here onwards we shall name the model samples by two letters that refer to the stock temperature and injection rate respectively, that is, LH corresponds to a sample processed at the lowest stock temperature and highest injection rate, etc.

### 2.2. Profilometry

Surface profile traces were measured with a Dektak 3030 mechanical profilometer. Ten traces of each sample were obtained, each consisting of 2000 equally spaced samples; the sampling interval was  $0.1 \mu\text{m}$ . The histograms, correlation functions and power spectra were estimated from these ten traces with the exception of sample run at the lowest stock temperature and highest injection speed (LH) where only three traces could be saved. To study the effects of a finite stylus tip, we implemented a computer simulation, in which the stylus tip is modeled as cone with a spherical tip. For this, we first generated numerically a one-dimensional surface profile with the required statistical properties. Then, we examine the path of a mathematically defined stylus as it moves laterally, in contact with the simulated profile. Although the deformation of the surface by weight loading is neglected, the simulation should provide an accurate representation of the actual measuring process. This simulation was performed for surfaces with Gaussian as well as truncated Lorentzian power spectra, and we found that the error in the estimation of both, the correlation length and the standard deviation of heights, is not significant. However, for surfaces with significant high spatial frequency components, such as one with an exponentially decaying correlation function, the finite stylus tip does affect the measurements. In this

case, one is unable to estimate the power spectrum correctly by mechanical profilometry.

Although the correlation functions and power spectra used to generate the scattering patterns were obtained by mechanical profilometry, for the sake of comparison we also characterized the surfaces by optical profilometry by means of a Wyko profilometer. This instrument has the advantage that it provides a two-dimensional array of data corresponding to the surface profile. The disadvantage of this technique is that the sample needs to be coated with a thin layer of highly reflecting materials (gold in our case) otherwise focusing errors, and light scattered by out-of-focus planes affect the measurements severely.

### 2.3. Light scattering

The angular distribution of the scattered light was measured with an automated scattering instrument, shown schematically in Fig. 1. The illumination was provided by a He-Ne laser ( $\lambda = 0.6328 \mu\text{m}$ ). To control the angle of incidence, the sample was mounted on a stage that allowed rotation about the vertical axis. The expanded laser beam passes through a periscope and follows along the horizontal plane of incidence towards the sample as shown in Fig. 1. A slightly converging beam was employed to concentrate the specular component to a very narrow region in the semicircle explored by the detector; for a perfectly flat surface the reflected beam was focused on the detector aperture. This arrangement was necessary to separate the diffuse and specular components. The detector was mounted on a 65 cm long arm that rotated about the sample in the horizontal plane. The measurements presented here thus represent the scattering in the plane of incidence. The exit periscope mirror blocked the detector when it was near the backscattering position and impeded measurements in that region. For the detection we used a photomultiplier and a picoammeter.

For a fixed angle of incidence, the scattered intensity was measured as a function of the scattering angle. To reduce the speckle noise, a 15 mm diameter sample area was illuminated and the scattered intensity was integrated over a fixed solid angle by means of a field lens and a detector. Ideally the field lens was much larger than a speckle, yet smaller than the structure present in the scattered

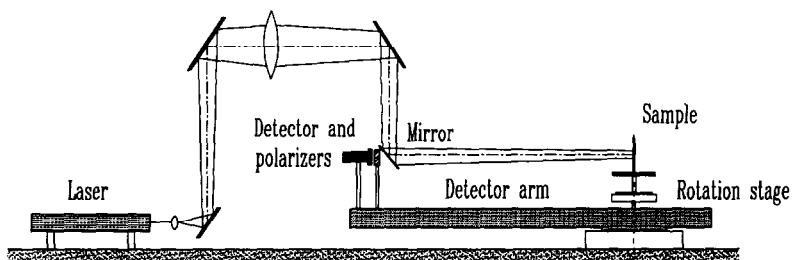


Fig. 1. Schematic representation of the light scattering apparatus.

field. Further, the field lens guaranteed that the detector viewed the entire illuminated area of the diffuser, irrespective of the angle of detection. A polarizer at the detector made it possible to measure the s- and p-polarization components of the scattered light. A small computer controlled the detector arm, so that data could be taken automatically.

### 3. Results and discussion

Figure 2 shows a typical scattering curve for an injection molded commercial ABS for polarization combinations, s-s and s-p, of the incident and scattered field respectively. The s-p pattern follows very closely a cosine dependence corresponding to a Lambertian scatterer that is typical of dense volume scattering. Moreover, when these samples were coated with gold, the absence of s-p scattering indicated that the surface did not contribute to the cross-polarized component. Therefore, we concluded that a scalar theory should be adequate in describing the scattering properties of such surfaces. On the other hand, the s-s curve shows a peak centered in the specular direction superimposed to an almost cosine background pattern. This implies that, at least approximately, the surface contribution could be separated from the volume contribution. For the model samples, due to the smaller particle volume fraction, the bulk contribution to scattering deviates slightly from a Lambertian. A proper comparison of the theory with experiments will require a knowledge of the angular distribution of the light scattered by the bulk near the specular angle. However for our samples the bulk contribution did not distort significantly the surface scattering curve around the specular angle.

For scattering in the plane of incidence, a surface with a Gaussian probability

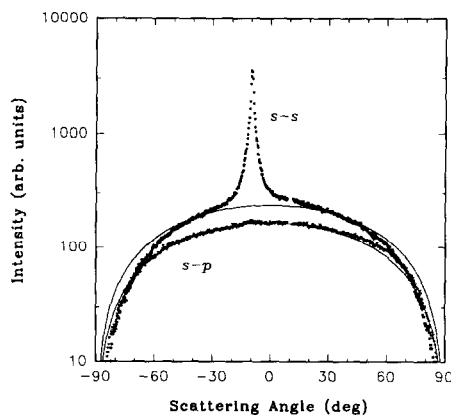


Fig. 2. Diffuse intensity as a function of the scattering angle of a typical commercially formulated ABS. The dashed lines represent the experimental data for s-s and s-p polarization combinations. The full lines correspond to a cosine dependence associated to a Lambertian scatterer.

density function of heights, and a detector-defined solid angle of the order of  $10^{-3}$  st (common in most commercial glossmeters), the diffuse scattered intensity can be calculated using a scalar theory based on the Kirchhoff approximation [6,7],

$$I(\mathbf{r})_{\text{incoh}} = \frac{2\pi A_M}{(\lambda r)^2} F^2(\theta_1, \theta_2) \exp(-g) \int_0^\infty J_0(v|r_1) \{ \exp[gC(r_1)] - 1 \} r_1 dr_1, \tag{1}$$

where

$$g = [2\pi(\sigma/\lambda)(\cos \theta_1 + \cos \theta_2)]^2, \tag{2}$$

$$F(\theta_1, \theta_2) = R_0 \frac{(\sin \theta_1 - \sin \theta_2)^2 + (\cos \theta_1 + \cos \theta_2)^2}{2(\cos \theta_1 + \cos \theta_2)}, \tag{3}$$

$$v = (2\pi/\lambda) (\sin \theta_1 - \sin \theta_2), \tag{4}$$

where  $\lambda$  is the wavelength of light,  $\sigma$  is the standard deviation of heights,  $R_0$  is the average reflectivity of the surface,  $A_M$  is the area of the mean surface,  $\theta_1$  is the angle of incidence and  $\theta_2$  is the scattered angle both measured with respect to the normal to the mean plane of the surface.  $J_0$  is the Bessel function of order zero and  $C(r)$  is the normalized correlation function of the height fluctuations. Therefore within the above assumptions, a model for gloss requires the knowledge of  $C(r)$  and  $\sigma$ .

On the other hand, the coherent component of the scattered light  $I_{\text{coh}}$ , will only depend of the probability density function of heights. For a Gaussian probability density function this reduces to [6,7]

$$I_{\text{coh}} = I_0 e^{-g}, \tag{5}$$

where  $I_0$  represents the intensity that would arise by reflection from a perfectly flat surface with reflectivity  $R_0$ . Using this expression,  $\sigma$  can be determined directly from measurements of the strength of the coherent component of the scattered light.

Table 1 summarizes the surfaces parameters found experimentally for the model systems by mechanical and optical profilometry, and using Eq. (5). We also

Table 1  
 $\sigma$  and  $\lambda_0$  for model samples determined by mechanical and optical profilometry and the strength of the coherent component.

Sample	Mechanical profilometry		Optical $\sigma$ ( $\mu\text{m}$ )	Coherent component $\sigma$ ( $\mu\text{m}$ )
	$\sigma$ ( $\mu\text{m}$ )	$\lambda_0$ ( $\mu\text{m}$ )		
LL	0.057	13	0.048	0.055
LH	0.047	14	0.035	0.047
HL	0.068	5.7	0.058	0.075
HH	0.039	15	0.028	

see from the table that the values of  $\sigma$  obtained by mechanical profilometry and by the strength of the coherent component match quite closely. Optical profilometry gives values of  $\sigma$  that are systematically below those obtained by the other methods.

As we mentioned earlier, to calculate the diffuse component of the scattered light from Eq. (1) we must know the correlation function  $C(r)$ , or equivalently its Fourier transform, the power spectrum. It is convenient to have a simple analytical form for  $C(r)$  that will reproduce, at least approximately, the experimental power spectrum. For this we choose the  $K$ -correlation function [8],

$$C_\nu(R) = (R/\xi)^\nu [2^{\nu-1} \Gamma(\nu)]^{-1} K_\nu(R/\xi), \quad (6)$$

that constitutes a family of functions that describes surface roughness with a wide range of textures. Here,  $K_\nu$  is the modified Bessel function of order  $\nu$ . For  $\nu = \frac{1}{2}$ , Eq. (6) reduces to a negative exponential, and for an integer  $\nu \gg 1$  it will take the form of a Gaussian. In these two cases,  $\xi$  will be identical to the correlation length  $\lambda_0$ , defined as distance for which the normalized correlation function decays to a value of  $1/e$ . These two limits correspond to a Brownian fractal and a single scale surface, respectively.

The procedure followed was to find the best value of  $\nu$  such that the power spectrum derived from Eq. (6) represented adequately the high spatial frequency zone of the corresponding profilometer data. Then the parameter  $\xi$  was adjusted so that the normalized correlation function decayed to  $1/e$  at a distance equal to the experimental correlation length. Using Eq. (1) together with the measured values of  $\sigma$  and  $\lambda_0$ , we calculated the diffuse scattering patterns for a decaying exponential, a Gaussian, and a  $K$ -correlation function, and compared these with the corresponding light scattering experiments.

Figures 3 and 4 show the measured and theoretical scattering patterns for samples HL and HH respectively. From these we see that the  $K$ -correlation function and the negative exponential correlation function, obtained by the procedure pointed out previously, give a reasonable description of the scattering pattern near the specular angle. However, as shown in Figs. 5 and 6, for samples LL and LH only the decaying exponential correlation function is in good agreement with the experimental scattering pattern around the specular angle. Gaussian correlation functions on the other hand do not predict the scattering behavior, even in the specular angular range. It is important to mention that, in order to fully separate surface from bulk scattering, all samples (except LL) were gold coated for this set of experiments. The fact that the scattering curve calculated with the  $K$ -correlation function does not agree with the experimental pattern, as one would expect, is probably due to the limitations of the mechanical profilometry in the high spatial frequency region as discussed above. From all this evidence one is inclined to believe that the actual correlation function is indeed close to a decaying exponential which suggests a multiscale surface roughness.

Within the particle migration model of surface formation [2,5]  $\sigma$  is determined

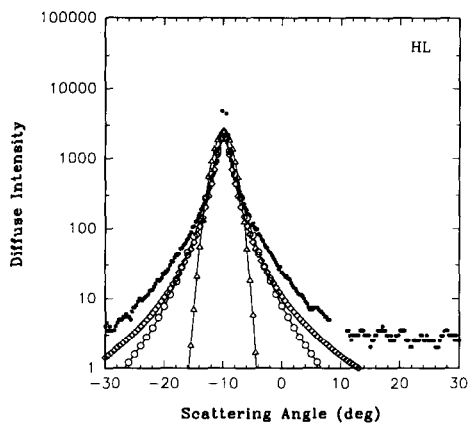


Fig. 3.

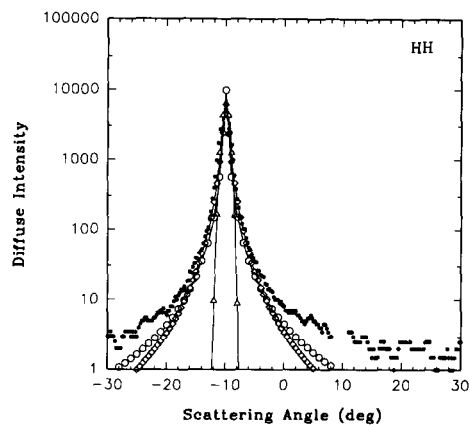


Fig. 4.

Fig. 3. Diffuse intensity as a function of the angle of scattering for sample HL gold-coated for an s-s incidence and detected polarization combination. The incidence angle is  $\theta_i = -10^\circ$ . The thick solid line represents the experimental data. The triangles and diamonds corresponds respectively to a Gaussian and negative exponential correlation function theoretically predicted scattering pattern with  $\sigma = 0.068 \mu\text{m}$  and  $\lambda_0 = 5.7 \mu\text{m}$ . The open circles represent the calculations with a Bessel  $K_\nu$  correlation function with  $\nu = 1$  and  $\xi = 3.44 \mu\text{m}$ .

Fig. 4. Diffuse intensity as a function of the angle of scattering for sample HH gold-coated for an s-s incidence and detected polarization combination. The incidence angle is  $\theta_i = -10^\circ$ . The thick solid line represents the experimental data. The triangles and diamonds correspond, respectively, to a Gaussian and negative exponential correlation function theoretically predicted scattering pattern with  $\sigma = 0.039 \mu\text{m}$  and  $\lambda_0 = 15 \mu\text{m}$ . The open circles represent the calculations with a Bessel  $K_\nu$  correlation function with  $\nu = 0.25$  and  $\xi = 29.24 \mu\text{m}$ .

by the particle size distribution, the mechanism of particle migration to the surface and smoothing at the mold wall. From optical- and electron-microscopy studies performed on these samples [5] there are strong indications that indeed the particles play an important role in the formation of the surface. Furthermore,  $\lambda_0$  is a measure of the bump extension, and it turns out to be of the same order of magnitude as the particle extension measured at the surface. The latter constitutes an additional evidence of the validity of the particle migration picture.

#### 4. Conclusions

We have shown that for injection molded particle filled polymers, a scalar theory based on the Kirchhoff approximation, with a Gaussian probability density of heights and a negative exponential correlation function between heights, predicts reasonably well the surface scattering properties in an angular interval around the specular angle. This leads to a simple analytical model for gloss with only two parameters,  $\sigma$  and  $\lambda_0$ . Therefore, if  $\sigma$  and  $\lambda_0$  can be calculated from process and materials variables, then gloss can be written in terms of such variables.

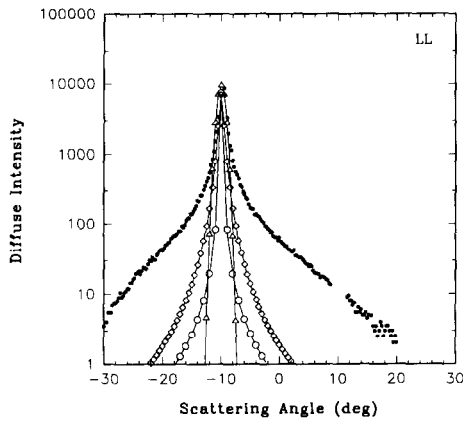


Fig. 5.

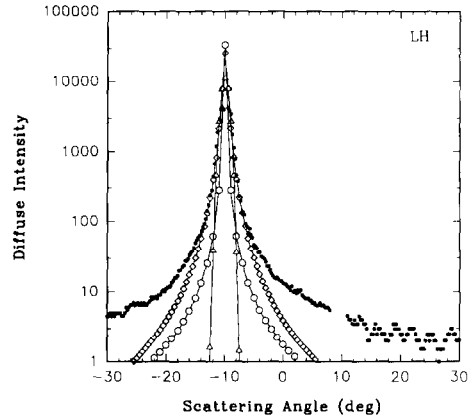


Fig. 6.

Fig. 5. Diffuse intensity as a function of the angle of scattering for sample LL for an s-s incidence and detected polarization combination. The incidence angle is  $\theta_i = -10^\circ$ . The thick solid line represents the experimental data. The triangles and diamonds correspond, respectively, to a Gaussian and negative exponential correlation function theoretically predicted scattering pattern with  $\sigma = 0.057 \mu\text{m}$  and  $\lambda_0 = 13 \mu\text{m}$ . The open circles represent the calculations with a Bessel  $K_\nu$  correlation function with  $\nu = 0.15$  and  $\xi = 51.18 \mu\text{m}$ .

Fig. 6. Diffuse intensity as a function of the angle of scattering for sample LH gold-coated for an s-s incidence and detected polarization combination. The incidence angle is  $\theta_i = -10^\circ$ . The thick solid line represents the experimental data. The triangles and diamonds correspond, respectively, to a Gaussian and negative exponential correlation function theoretically predicted scattering pattern with  $\sigma = 0.047 \mu\text{m}$  and  $\lambda_0 = 14 \mu\text{m}$ . The open circles represent the calculations with a Bessel  $K_\nu$  correlation function with  $\nu = 0.15$  and  $\xi = 55.12 \mu\text{m}$ .

## Acknowledgements

We would like to express our gratitude to Industrias Resistol S.A. for their financial support to this project. We also are grateful to Monsanto Co. for all the facilities received by one of us (R.A.-K.) in processing the samples used in this work, as well as, for the electron-microscope studies on them. In particular we would like to thank Richard Hoffman for all his scientific advice and Frank Silver for his invaluable logistic support.

## References

- [1] L. Fritch *Plast. Eng.* 35 (1979) 68.
- [2] R.L. Hoffman, in: *Advances in Rheology, 2. Fluids*, Proc. IX Intern. Congress on Rheology (1984) p. 565.
- [3] R.L. Hoffman, *J. Rheol.* 29 (1985) 579.
- [4] J.A. Stoos and L.G. Leal, *AIChE J.* 35 (1989) 196.
- [5] R.L. Hoffman, R. Alexander-Katz, R. López B. and O. Manero, work in progress.



- [6] P. Beckmann and A. Spizzichino, *Scattering of Electromagnetic Waves from Rough Surfaces* (Pergamon, London, 1963).
- [7] J.A. Ogilvy, *Theory of Wave Scattering from Random Rough Surfaces* (Adam Hilger, Bristol, 1991).
- [8] B.J. Hoenders, E. Jakeman, H.P. Baltes and B. Steinle, *Opt. Acta* 26 (1979) 1307.